Supplementary Information

Self-driven approach for local ion intercalation in vdW crystals

Haojie Lai [a], Ruihui He [a], Xin Xu [a], Tingting Shi* [a], Xi Wan[c], Hui Meng [a], Ke Chen [a], Yang Zhou [a], Qiulan Chen* [b], Pengyi Liu [a], Jian Chen[d], Jianbin Xu [e,f], Weiguang Xie* [a,e]

[a] Guangdong Provincial Key Laboratory of Optical Fiber Sensing and Communications, and Siyuan Laboratory, Guangdong Provincial Engineering Technology Research Center of Vacuum Coating Technologies and New Energy Materials, Department of Physics, Jinan University, Guangzhou, Guangdong 510632, People's Republic of China

[b] Department of Medical Devices, Guangdong Food and Drug Vocational College, Guangzhou 510520, People's Republic of China

[c] Engineering Research Center of IoT Technology Applications (Ministry of Education), Department of Electronic Engineering, Jiangnan University, Wuxi, Jiangsu 214122, People's Republic of China

[d] Instrumental Analysis & Research Center, Sun Yat-sen University, Guangzhou 510275, People's Republic of China

[e] State Key Laboratory of Optoelectronic Materials and Technologies, Sun Yat-sen University, Guangzhou 510275, People's Republic of China

[f] Department of Electronic Engineering and Materials Science and Technology Research Center, The Chinese University of Hong Kong, Hong Kong SAR, China

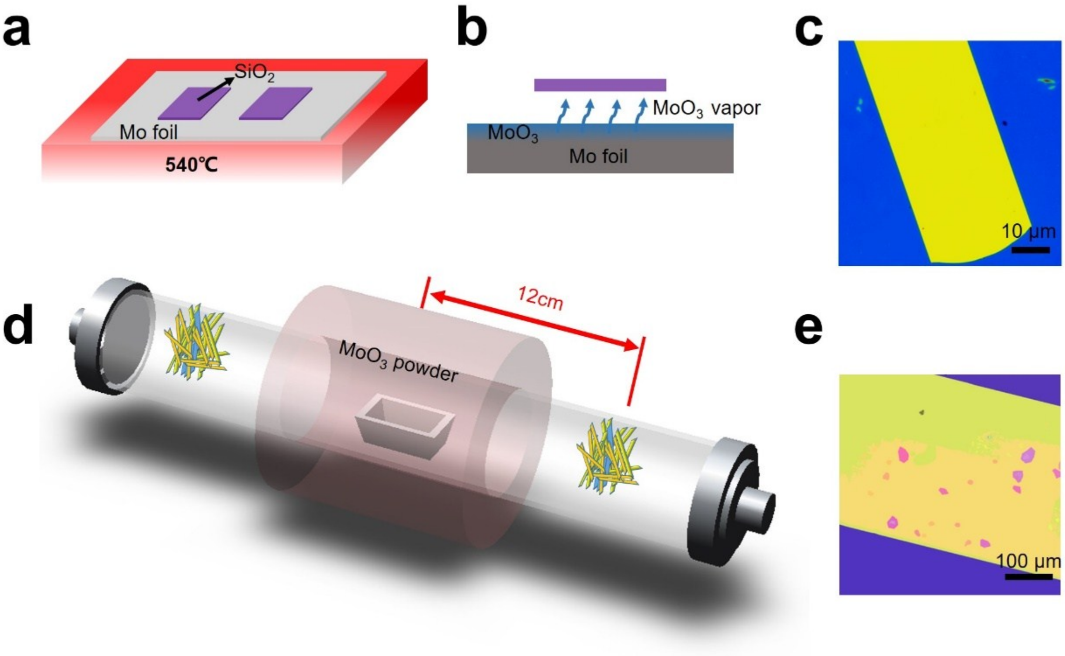

Figure S1 (a) & (b) Schematic illustration of hot-plate method to prepare MoO_3 nanosheets. (c) The optical image of the MoO_3 flakes. (d) PVD growth of MoO_3 single crystal. (e) The image of mass-produced MoO_3 single crystal

The MoO_3 in our experiment was prepared in two ways. The first was hot-plate method (Fig. S1a-c). In this method, a hot plate was heated to 540 °C and kept for a 10 minutes in atmosphere. A SiO_2/Si substrate was placed on a Mo foil with the SiO_2 facing down. It was then placed on the hot-plate for 2-5 mins. The Mo foil was oxidized and the MoO_3 nanosheet was deposited on the substrate. The sample was then was taken out and cooled in air.

The second way was physical vapor deposition (PVD) preparation of MoO_3 single crystals (Fig. S1d&e). It involved the following steps: 0.3g MoO_3 powder was placed in the middle of the heating zone of the tube furnace. The tube was heated to 780 °C and held for 1 hour, and then naturally cooled down. High quality MoO_3 single crystal was deposited on the tube wall at a distance of 12 cm away from the powder source.

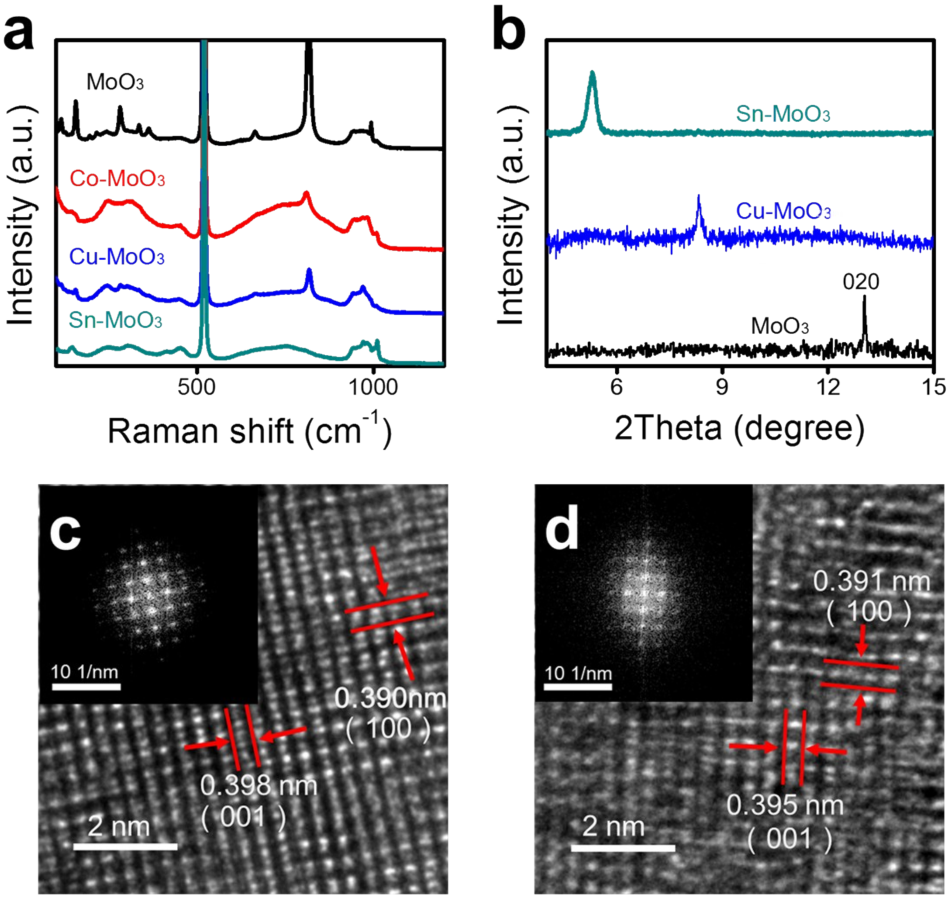

Figure S2 (a) Raman spectra of MoO_3, Co-MoO_3 Cu-MoO_3 and Sn-MoO_3. (b) XRD diffraction pattern of MoO_3, Cu-MoO_3 and Sn-MoO_3. (c) & (d) TEM diffraction images of Cu-MoO_3 and Sn-MoO_3. The insets show the corresponding SAED patterns. The intercalation concentration is 1×10^{-3} M

For Cu intercalation, 0.1 g $Cu(NO_3)_2$ powder (99.9% purity) was dissolved in 60 ml deionized water to obtain 10 mM $Cu(NO_3)_2$. For Sn intercalation, 0.15 g $SnCl_4$ powder (99.9% purity) was dissolved in 60 ml deionized water to obtain 10 mM $SnCl_4$. The solution was then diluted to desired concentration.

Intrinsic MoO_3 shows a Raman peak at 820 cm^{-1} originated from the O_3–Mo–O_3 stretching vibration along the [100] direction, and a small peak at 993 cm^{-1} due to the

Mo-O_1 vibration along [010] direction (Fig. S2a). After intercalation of Co, Cu or Sn ions, the intensity of the in-plane O_1–Mo–O_3 vibration significantly reduced, while the intensity of out-of-plane Mo-O_1 vibration changes slightly. It means that molecular layers are relaxed along the [010] directions so that it is slightly affected by the vdW gap intercalation. This relaxation cause the expansion along *b* axis as shown in Fig. S2b. All intercalated MoO_3 crystals show additional peaks at smaller angles. These peaks appear at different positions, which means that the expansion varies due to different interaction between the ion and the MoO_3.

The Sn and Cu intercalated sample show peaks at different positions, which means that the expansion of lattices is different. The (020) peak of MoO_3 is missing because the MoO_3 is fully intercalated. It should be noted that XRD require macro scale sample, while our method is not good at large scale intercalation. The intensity of the peaks can not be compared directly here because the amount of MoO_3 sample is small and there is great difference between samples. Both TEM images in Fig. S2c & d confirm significant lattice expansion along the [001] direction, which are consistent with that of Co-MoO_3. Disorder effect in the Sn-MoO_3 is stronger than the other two sample as shown by the blur diffraction spot in the SAED pattern. It shows that the intercalation effect depends on intercalation ion types.

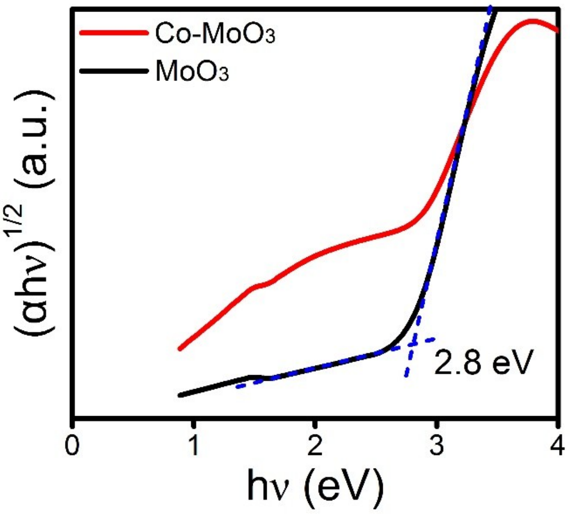

Figure S3 Optical band gap extraction of MoO_3 from Fig. 3a. The intercalated sample shows large gap states that narrow the optical gap. It's not able to extract its optical gap due to the measurement limit.

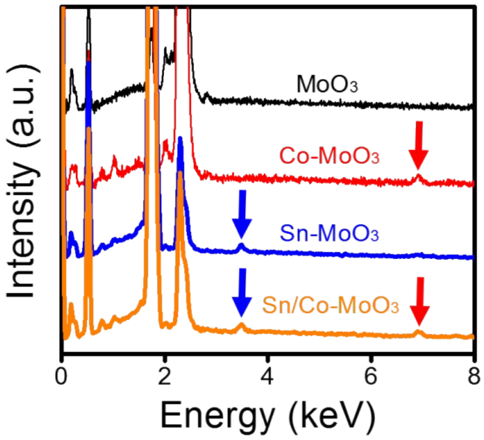

Figure S4 Energy dispersive spectroscopy (EDS) on different regions of MoO_3 nanosheets in **Fig. 4**. The red arrow indicates the peak of Co element and the blue arrow for Sn element. The atomic contents of Sn and Co are small. They can be determined roughly as $Co_{0.13}MoO_3$, $Sn_{0.05}MoO_3$, and $Co_{0.8}Sn_{0.2}MoO_3$. The Co content is higher than the Sn in single intercalated region.

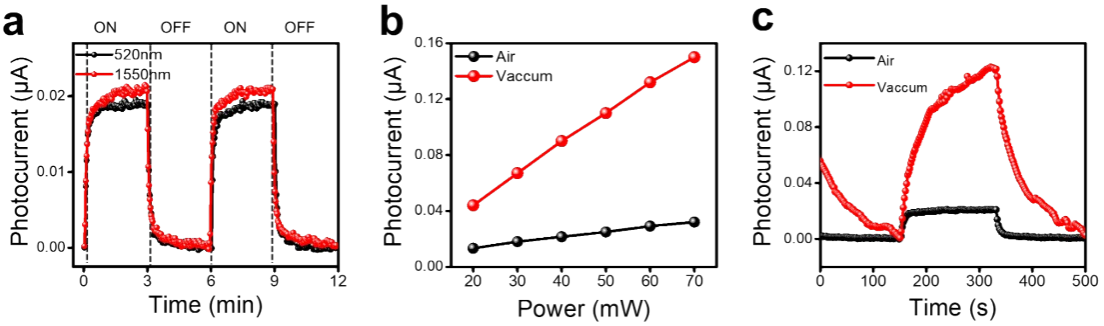

Figure S5 Broadband photoresponse of a Co-intercalated MoO_3 photoconductive device. (a) Transient photoresponse at a bias voltage of 0.1 V under 50 mW laser power in air under 520 nm and 1550 nm excitation. (b) Power dependence of photocurrent in air and vacuum under illumination of 1550 nm. (c) Photoresponse under air and vacuum condition.

Intrinsic MoO_3 shows no response to visible light, while the intercalated MoO_3 nanosheet shows broadband photoresponse to illumination wavelength of 520 nm and 1550 nm (Fig. S5a). The rise/decay response time under atmosphere is 21.8 s/27.0 s. Fig. S5b shows that the photocurrent linearly increases with increasing illumination power, giving a responsivity of 0.02 AW^{-1} in air at 1550 nm. Photocurrent under vacuum condition is several times higher than that in air, giving a responsivity of 0.12 AW^{-1}. However, the rise/decay time is as slow as 1.82 min/1.88 min. This implies that there are localized states in the Co-intercalated MoO_3.

The difference of photo-current between vacuum and air is associated with the oxygen adsorption effect on the metal oxides. In an oxygen-rich atmosphere, oxygen molecules capture electrons from the surface of metal oxide, resulting in the formation of oxygen anion [$O_2(g) + e^- \rightarrow O_2^-(ad)$] layer on the surface. This effect causes a surface depletion layer. Under illumination, the excited electrons will be trapped by the surface layer, and leads to the decrease of photo-conductivity. In vacuum condition, the adsorbed oxygen molecules will be desorbed, which reduces the depletion effect. Therefore, the photocurrent is vacuum is higher than that in air.

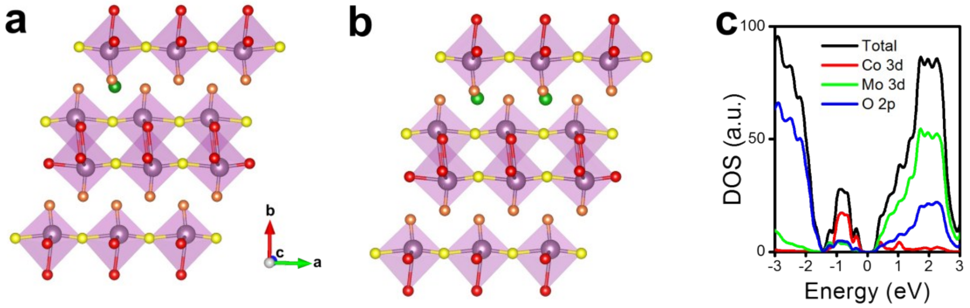

Figure S6 (a) The most stable intercalated site in MoO_3 for Sn or Co atom. (b) Two intercalated atoms in the cell. (c) The calculated DOS of intercalated MoO_3 with two Co atoms in (b).

The crystal structure of α-MoO_3 is composed of the distorted octahedral units, and each layer is connected through van der Waals interaction. There are three coordinated oxygen atoms in MoO_3, represented by three different colors in Fig. S6 a&b. Our calculation shows that the interstitial site between two layers are the most stable intercalated site due to the large space of the van der Waals gap. The DOS was then calculated by assuming the intercalated atoms in the vdW gap.

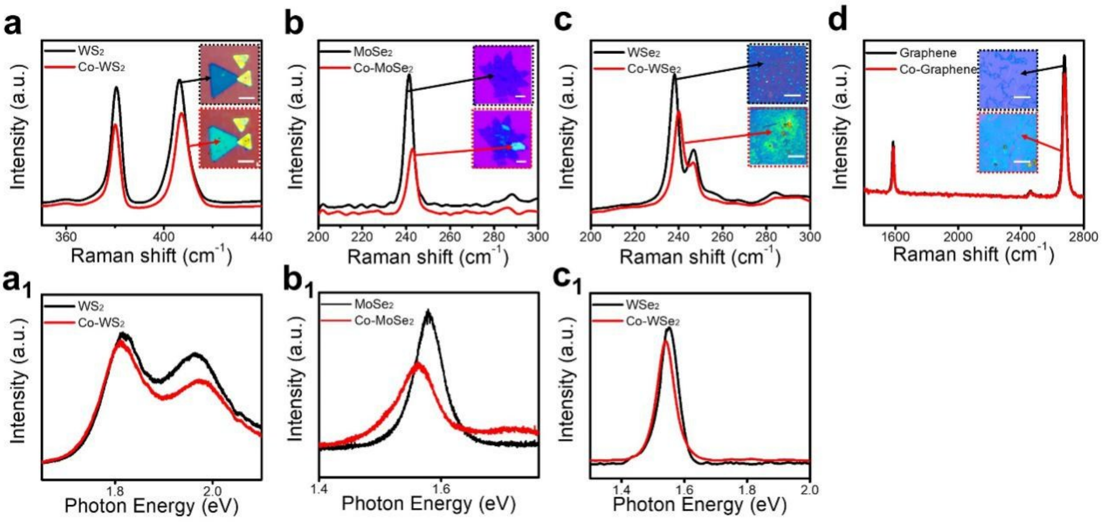

Figure S7 (a)-(d) Raman spectra of WS_2 and Co-WS_2 nanosheet, $MoSe_2$ and Co-$MoSe_2$ nanosheet, WSe_2 and Co-WSe_2 nanosheet and graphene and Co-graphene respectively. (a_1)-(c_1) Corresponding photoluminescence spectra of WS_2 and Co-WS_2 nanosheet, $MoSe_2$ and Co-$MoSe_2$ nanosheet, WSe_2 and Co-WSe_2 nanosheet in (a)-(c) respectively.

All the 2D materials are grown by chemical vapor deposition. To prepare graphene, Cu foils was annealed at 1000 °C in forming gas (20% H2 + 80% Ar) at a pressure of 10^{-4} Torr. Triphenylene was introduced to the foil through electrical resistance heating at a vapor pressure of 10^{-5} Torr. After a 30 min reaction, the Cu foil was cooled down to room temperature at a base pressure of 10^{-7} Torr. The graphene was then transferred to SiO2 surface for intercalation. To prepare MoS_2/$MoSe_2$/WS_2/WSe_2 Sulfur/selenium powder (≈0.5 - 1 g) and MoO_3/WO_3 powder (Alfa Aesar, 99.9995%, 5 - 50 mg) were put in different temperature zone of a homemade glass container with a long, narrow output tube (OD ≈ 3 mm). 300 nm - thick SiO_2/Si substrates (1 cm × 1 cm) were placed downstream relative to the Ar gas (500 sccm) flow direction. The sulfur was evaporated by a heating belt at 120–150 °C, and 250 °C for selenium. The amount of sulfur/selenium could be well controlled/reduced with the help of the narrow output tube. The growth temperature was raised to ≈800 – 900 ° C to further enable the reaction between MoOx/Wox flakes with S/Se for crystalline sample for 0.5 – 3 h. Finally, the system was naturally cooled down to room temperature. More detail growth parameters of graphene, MoS_2, WS_2 $MoSe_2$ and WSe_2 and can be found in previous publications in Ref.[1-4].

For cobalt ion intercalation in other 2D materials, 0.1 g $CoSO_4$ powder (99.9 % purity) was dissolved in 60 ml deionized water to obtain 10 mM $CoSO_4$ solution. The solution was then diluted to desired concentration. Zn powder (99.9 % purity) with diameter of around 10 μm was dispersed on the surface of WS_2, $MoSe_2$, WSe_2 and graphene nanosheet. A drop of $CoSO_4$ solution was dropped onto the nanosheet. Intercalation was observed under an optical microscope. After intercalation, the nanosheets showed distinct color change relative to the intrinsic ones. The change of Raman spectra and photoluminescence spectra was shown in Fig. S7.

It's clear that first, the color of the 2D materials change after intercalation. The reduction of Raman intensity are close to what has been observed in MoS_2. It implies that intercalation has altered the interlayer coupling. The reduction of PL intensity gives the support.

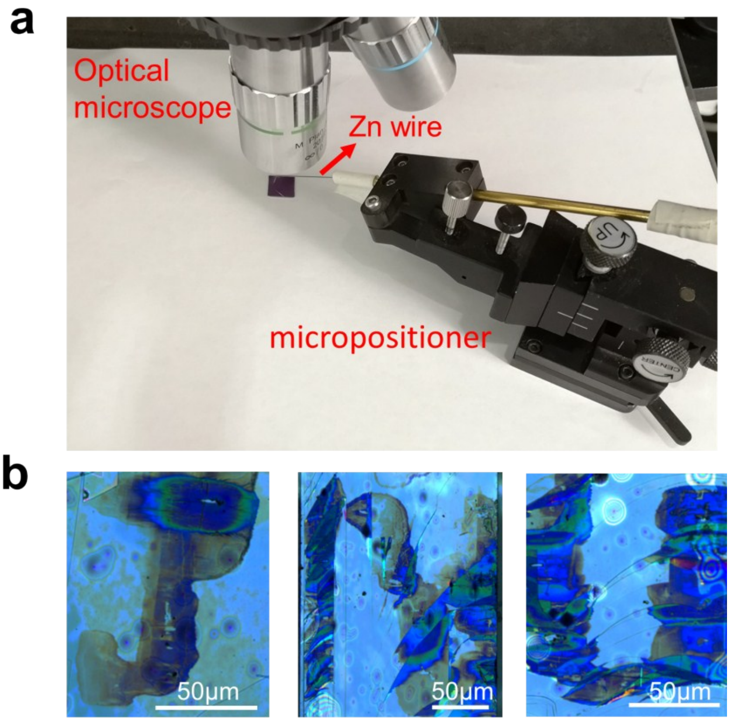

Figure S8 (a) Apparatus to realize local intercalation. (b) Optical image of "JNU" by Co intercalation on a single crystal MoO_3 using a Zn wire.

The Zn wire is fixed on a micropositioner with accuracy of 5 μm (Fig. S8a). The wire is brought by the micropositioner into contact with the surface of the MoO_3 under an optical microscope. The intercalation process can be monitored under the optical microscope.

1 K. Chen, X. Wan, D. Liu, Z. Kang, W. Xie, J. Chen, Q. Miao, and J. Xu, Nanoscale **5** (13), 5784-5793 (2013).

2 X. Wan, K. Chen, W. Xie, J. Wen, H. Chen, and J.-B. Xu, Small **12** (4), 438-445 (2016).

3 Y.H. Chang, W. Zhang, Y. Zhu, Y. Han, J. Pu, J.K. Chang, W.T. Hsu, J.K. Huang, C.L. Hsu, M.H. Chiu, T. Takenobu, H. Li, C.I. Wu, W.H. Chang, A.T. Wee, and L.J. Li, ACS Nano **8** (8), 8582-8590 (2014).

4 J.-K. Huang, J. Pu, C.-L. Hsu, M.-H. Chiu, Z.-Y. Juang, Y.-H. Chang, W.-H. Chang, Y. Iwasa, T. Takenobu, and L.-J. Li, ACS Nano **8** (1), 923-930 (2013).